Particle Dark Matter Searches Outside the Local Group

Marco Regis,[1,*] Jun-Qing Xia,[2,†] Alessandro Cuoco,[1,‡] Enzo Branchini,[4,5,6] Nicolao Fornengo,[1] and Matteo Viel[7,8]
[1]*Dipartimento di Fisica, Università di Torino and Istituto Nazionale di Fisica Nucleare, Sezione di Torino, via Pietro Giuria 1, I-10125 Torino, Italy*
[2]*Key Laboratory of Particle Astrophysics, Institute of High Energy Physics, Chinese Academy of Science, P.O. Box 918-3, Beijing 100049, People's Republic of China*
[3]*Dipartimento di Matematica e Fisica, Università degli Studi "Roma Tre", via della Vasca Navale 84, I-00146 Roma, Italy*
[4]*INFN, Sezione di Roma Tre, via della Vasca Navale 84, I-00146 Roma, Italy*
[5]*INAF Osservatorio Astronomico di Roma, INAF, Osservatorio Astronomico di Roma, Monte Porzio Catone, Italy*
[6]*INAF Osservatorio Astronomico di Trieste, Via Giovanni Battista Tiepolo 11, I-34141 Trieste, Italy*
[7]*INFN, Sezione di Trieste, via Valerio 2, I-34127 Trieste, Italy*
(Received 20 March 2015; published 16 June 2015)

If dark matter (DM) is composed by particles which are nongravitationally coupled to ordinary matter, their annihilations or decays in cosmic structures can result in detectable radiation. We show that the most powerful technique to detect a particle DM signal outside the Local Group is to study the angular cross-correlation of nongravitational signals with low-redshift gravitational probes. This method allows us to enhance the signal to noise from the regions of the Universe where the DM-induced emission is preferentially generated. We demonstrate the power of this approach by focusing on GeV-TeV DM and on the recent cross-correlation analysis between the 2MASS galaxy catalogue and the Fermi-LAT γ-ray maps. We show that this technique is more sensitive than other extragalactic γ-ray probes, such as the energy spectrum and angular autocorrelation of the extragalactic background, and emission from clusters of galaxies. Intriguingly, we find that the measured cross-correlation can be well fitted by a DM component, with a thermal annihilation cross section and mass between 10 and 100 GeV, depending on the small-scale DM properties and γ-ray production mechanism. This solicits further data collection and dedicated analyses.

DOI: 10.1103/PhysRevLett.114.241301 PACS numbers: 95.35.+d, 95.80.+p, 98.70.Rz, 98.70.Vc

Introduction.—The origin of cosmic structures is well understood in terms of evolution of matter perturbations arising after the inflationary period. Inhomogeneities starting off with higher-than-average density grow through gravitational instability. Dark matter (DM) is a necessary ingredient to the process, as it provides the potential wells where standard matter is accreted after decoupling and protohalos form. As structure formation evolves, DM halos of increasing size form in a bottom-up fashion.

If DM is in the form of particles which exhibit non-gravitational couplings to ordinary matter, a certain level of emitted radiation is expected. Photons can be produced from interactions of DM with the ambient medium (e.g., through scatterings) or from DM annihilation or decay by means of direct emission or through the production of intermediate particles. The nongravitational signal associated to decay is proportional to the DM density: it is stronger at low redshift, because the produced radiation is diluted by the expansion of the Universe more rapidly than its source, i.e., the DM particle density. The DM annihilation signal, which is proportional to the density squared, is also peaked at low redshift since the density contrast associated to cosmic structures grows nonlinearly.

DM constitutes the backbone of all cosmic structures and DM halos represent, collectively, a potential source of DM decay or annihilation signals. This means that even if the radiation originating from DM annihilations or decays in a single halo is too faint to be detected, their *cumulative signal* and its *spatial coherence* could be. In addition, since the DM signal is expected to peak at $z < 0.3$, it can be separated by more mundane astrophysical processes that typically trace the star formation history and peak at higher redshifts.

To increase the sensitivity to nongravitational DM sources, one needs to isolate the annihilation or decay signal produced at low redshift. An effective way to filter out any signal that is not associated to DM-dominated structures or that is originated at high redshift is to *cross-correlate* the radiation field with *bona fide* low-redshift DM tracers [1–6]. In the following, we adopt this approach in the specific and yet very relevant framework of weakly interacting massive particles (WIMP) that may either annihilate or decay. We will use the results of the cross-correlation analysis between γ-ray maps from Fermi-LAT [7] and the 2MASS catalogue of relatively nearby galaxies [8] presented in [9].

Data and models.—The cross angular power spectrum (CAPS) between the *unresolved* γ-ray sky observed by Fermi-LAT and the distribution of 2MASS galaxies can be written as [3]

$$C_\ell^{(\gamma g)} = \int \frac{d\chi}{\chi^2} W_\gamma(\chi) W_g(\chi) P_{\gamma g}(k = \ell/\chi, \chi), \quad (1)$$

where $\chi(z)$ denotes the radial comoving distance, $W_i(\chi)$ represents the window functions described below, $P_{\gamma g}(k, z)$ is the three-dimensional cross power spectrum (PS), k is the modulus of the wave number, and ℓ is the multipole. Indices γ and g refer to γ-ray emitters and extragalactic sources in 2MASS, respectively. In Eq. (1) we used the Limber approximation [10], since $P_{\gamma g}$ varies (relatively) slowly with k.

The (differential in energy) window function for γ-ray emission from DM annihilation $W_\gamma(z)$ is [3]

$$W_\gamma^a(z) = \frac{(\Omega_{\rm DM}\rho_c)^2 \langle \sigma_a v \rangle}{8\pi {m_{\rm DM}}^2} (1+z)^3 \Delta^2(z) \frac{dN_a}{dE_\gamma} e^{-\tau[z, E_\gamma(z)]}, \quad (2)$$

where $\Omega_{\rm DM}$ is the DM mean density in units of the critical density ρ_c, $\Delta^2(z)$ is the clumping factor, $m_{\rm DM}$ is the mass of the DM particles, and $\langle \sigma_a v \rangle$ denotes the velocity-averaged annihilation rate. A six-parameter flat Λ cold dark matter cosmological model is assumed with the value of the parameters taken from Ref. [11]. dN_a/dE_γ indicates the number of photons produced per annihilation and determines the γ-ray energy spectrum. The exponential damping quantifies the absorption due to extragalactic background light [12].

The window function for DM decay is [3]

$$W_\gamma^d(z) = \frac{\Omega_{\rm DM}\rho_c \Gamma_d}{4\pi m_{\rm DM}} \frac{dN_d}{dE_\gamma} e^{-\tau[z, E_\gamma(z)]}, \quad (3)$$

where $\Gamma_d = 1/\tau_d$ is the DM decay rate.

The window function of 2MASS galaxies is $W_g(z) \equiv H(z)/c dN_g/dz$ and their redshift distribution dN_g/dz is [13]

$$\frac{dN_g}{dz}(z) = \frac{\beta}{\Gamma(\frac{m+1}{\beta})} \frac{z^m}{z_0^{m+1}} \exp\left[-\left(\frac{z}{z_0}\right)^\beta\right], \quad (4)$$

with $m = 1.90$, $\beta = 1.75$, and $z_0 = 0.07$.

We employed the 2MASS catalogue instead of other compilations because the galaxy distribution in Eq. (4) is peaked at very low redshift as for the DM emission of Eqs. (2) and (3). This enhances the cross-correlation signal. The picture for astrophysical components would be different and other catalogues might be more informative (see Sec. S2 in the Supplemental Material [14]).

The PS $P_{\gamma g}$ in Eq. (1) is computed within the halo-model framework, as the sum of one-halo plus two-halo terms. For more details, see [3]. Both the PS and the clumping factor $\Delta^2(z)$ in Eq. (2) depend on a number of DM properties: the halo mass function, that we take from Ref. [22], the halo density profile, for which we assume a Navarro-Frenk-White model [23], the minimum halo mass, that we set equal to $10^{-6} M_\odot$, and the halo mass-concentration relation $c(M, z)$, that we adopt from Ref. [24]. The theoretical uncertainty of these quantities is rather small for halos larger than $10^{10} M_\odot$, because they can be constrained by observations and simulations. Since the DM decay signal is mainly contributed by large structures, the theoretical predictions are relatively robust. This is not the case for the annihilation signal which is preferentially produced in small halos and in substructures within large halos. Consequently, theoretical uncertainties on the annihilation signal are larger. For the subhalo contribution we consider two scenarios (LOW and HIGH) to bracket theoretical uncertainty. The LOW case follows the model of Ref. [25] [see their Eq. (2), with a subhalo mass function $dn/dM_{\rm sub} \propto M_{\rm sub}^{-2}$]. The HIGH scenario is taken from Ref. [26], with the halo mass-concentration relation extrapolated down to low masses as a power law. Further uncertainties in the concentration parameter and in the value of the minimum halo mass can introduce an extra factor of $\sim$2 of uncertainty, that we quantify only in the Supplemental Material [14], for the sake of definiteness.

In our CAPS model [Eq. (1)], we add a constant term C_{1h} (*one-halo correction term*) to correct for possible unaccounted correlations at very small scales, within the Fermi-LAT point spread function. The value of C_{1h} will be determined by fitting the data, and we anticipate that we find a C_{1h} value compatible with zero. Thus, the inclusion of this term does not change significantly the results. For a discussion on this term, see Ref. [5].

The measured CAPS $\tilde{C}_\ell^{(\gamma g)}$ is a convolution of the true CAPS and the effective beam window function W_ℓ^B that accounts for the point spread function of the instrument and the pixelization of the γ-ray map. Both quantities depend on energy. We use the W_ℓ^B derived in Ref. [9] and model the observed spectrum as $\tilde{C}_\ell^{(\gamma g)} = W_\ell^B C_\ell^{(\gamma g)}$.

In the following, we shall consider the angular cross-correlation function (CCF) rather than the spectrum. To model the CCF, we Legendre transform the CAPS:

$$\mathrm{CCF}^{(\gamma g)}(\theta) = \sum_\ell \frac{2\ell+1}{4\pi} \tilde{C}_\ell^{\gamma g} P_\ell(\cos(\theta)), \quad (5)$$

where θ is the angular separation and P_ℓ are the Legendre polynomials.

To compare model and observed CCFs, we estimate the χ^2 difference defined as

$$\chi^2 = \sum_{n=1}^{3} \sum_{\theta_i \theta_j} [d_{\theta_i}^n - m_{\theta_i}^n(\boldsymbol{A})] [C^n]^{-1}_{\theta_i \theta_j} [d_{\theta_j}^n - m_{\theta_j}^n(\boldsymbol{A})], \quad (6)$$

where m and d indicate model and data, n identifies each one of the three overlapping energy ranges considered

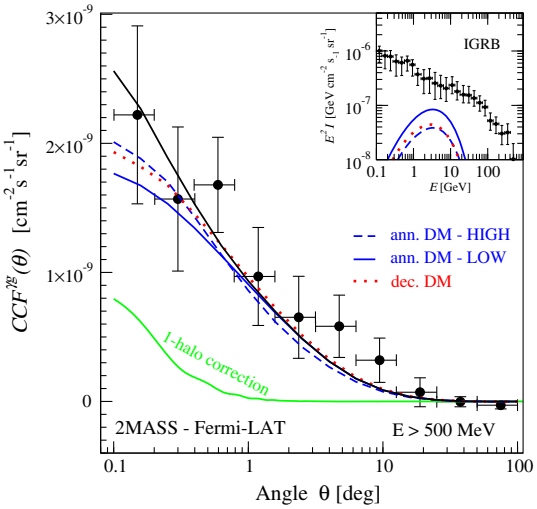

FIG. 1 (color online). Cross-correlation above 500 MeV for the best fitting annihilating and decaying DM scenarios, compared to the measured CCF. The curves are for DM particles of 100 GeV (200 GeV) annihilating (decaying) into $b\bar{b}$. We show the two annihilation models, HIGH and LOW, with annihilation rates $\langle\sigma_a v\rangle = 2\times10^{-26}$ cm^3 s^{-1} (blue-dashed curve) and 2.4×10^{-25} cm^3 s^{-1} (blue-solid curve), respectively, and a decay model with lifetime $\tau = 1.6\times10^{27}$ s (red-dotted curve). The green curve shows the CCF of the one-halo correction term C_{1h}. We show the sum of this component and the DM CCF (in the LOW scenario) with the black curve. The inset shows that these DM models provide a subdominant contribution to the observed IGRB spectrum [27].

($E > 0.5$, 1, and 10 GeV), and the indices θ_i and θ_j run over 10 angular bins logarithmically spaced between $\theta = 0.1°$ and 100°. $C^n_{\theta_i\theta_j}$ is the covariance matrix that quantifies the errors of the data and their covariance among the angular bins. Data and covariance matrix are taken from Ref. [9]. The parameter vector for annihilating DM is $\boldsymbol{A} = (m_{\rm DM}, \langle\sigma_a v\rangle, C_{1h})$, whereas for the decaying DM it is $\boldsymbol{A} = (m_{\rm DM}, \tau_d, C_{1h})$.

Results.—In Fig. 1 we show a comparison between the measured CCF in one of the considered energy bins ($E > 500$ MeV) and the best fitting annihilating and decaying DM models obtained from the analysis discussed below. Error bars are given by the diagonal elements of the covariance matrix. DM models fit the measured CCF remarkably well (for the best fitting model, $\chi^2_{\rm BF} = 16.7$ with 26 d.o.f.). It is also noteworthy that the level of annihilation or decay rate provides a minor contribution to the isotropic gamma-ray background (IGRB) measured by the Fermi-LAT [27], as shown in the inset of the figure. This implies that the cross-correlation technique can detect DM signals too faint to show up in the total intensity measurement (for a review of the IGRB properties, see Ref. [28]).

In Fig. 2, we show the 1σ and 2σ C.L. contours (obtained marginalizing over C_{1h}) for DM mass and annihilation or decay rate for various final states. Note that, although we use only three energy bins, they are sufficient to constrain the DM mass which induces a small but characteristic signature in the energy spectrum. In the LOW scenario the 1σ region lies just above the thermal annihilation rate $\langle\sigma_a v\rangle = 3\times10^{-26}$ cm^3 s^{-1}. In the HIGH case, the DM signal increases by a factor of $\sim$10 and consequently regions shift down by 1 order of magnitude. Therefore, given the current uncertainty in modeling DM structures we conclude that the thermal cross section is well within the allowed regions for $m_{\rm DM} \lesssim 200$ GeV.

We stress that the confidence contours in Fig. 2 are drawn under the assumption of no contribution from astrophysical sources. While their purpose is mainly illustrative, they may not be unrealistic since astrophysical sources, which are indeed required to account for the IGRB thanks to their medium-to-large redshift emission, can indeed provide a negligible contribution to the cross-correlation signal between Fermi-LAT and 2MASS galaxies that, as we point out, has a rather local origin (see the discussion in Sec. S2 of the Supplemental Material [14]). On the other hand, given the current uncertainty on the astrophysical components of the IGRB, an astrophysical model that can explain the measured cross-correlation signal with no additional contribution from DM can be found [9]. Future data and analyses will help distinguishing between these two options.

This cross-correlation measurement can alternatively be used to derive 95% C.L. upper bounds on the annihilation or decay rate. These bounds are conservative and robust, since we assume here that DM is the only source of the γ-ray signal, without introducing additional assumptions on astrophysical components which would make the constraints stronger but also more model dependent. The 95% C.L. upper bounds on the WIMP annihilation (decay) rate as a function of WIMP mass are shown in the left-hand (right-hand) panel of Fig. 3. For $b\bar{b}$ and $\tau^+\tau^-$ final states, the thermal annihilation rate is excluded for masses below 10 (100) GeV in the LOW (HIGH) scenario. In the case of $\mu^+\mu^-$, the bounds degrade by about 1 order of magnitude.

In Fig. 4 we compare the sensitivity of our cross-correlation method with that of other *extragalactic* γ-ray probes. We focus on these probes since they are similarly affected by uncertainties in modeling DM halo and subhalo properties. This allows us to compare various techniques in a homogeneous and robust way, something that cannot be done with local DM tracers (galactic regions, dwarf galaxies) or early Universe probes, which have different systematic uncertainties (see, however, the discussion in Sec. S1 of the Supplemental Material [14]). For illustrative purposes, we selected the LOW substructure scheme and $b\bar{b}$ final states case. We verified that different choices provide little differences and the results are robust to both the DM clustering model and the annihilation or decay channel. We consider again the simplest case (where most conservative bounds can be derived), in which the astrophysical

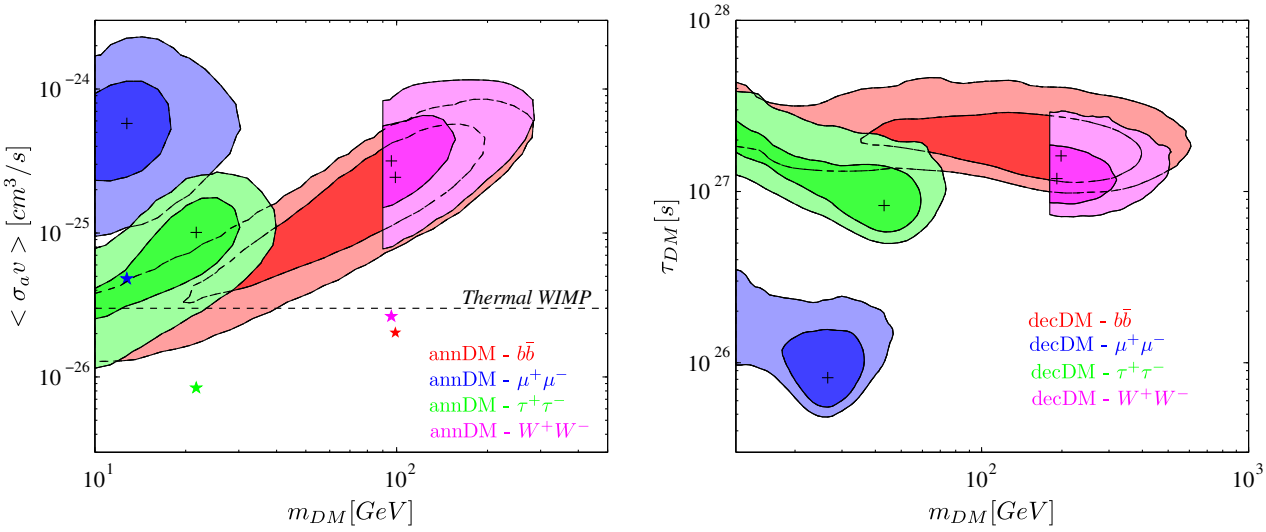

FIG. 2 (color online). Left: 1σ and 2σ allowed regions for the DM annihilation rate versus its mass, for different γ-ray production channels and assuming a LOW substructure scheme. Crosses indicate the best fitting models. In the HIGH scenario, regions remain similar but shifted downward by a factor of $\sim$12; see stars indicating the best fitting models. Right: The same as in the left-hand panel but for decaying DM, showing the DM particle lifetime as a function of its mass.

contribution is set to zero in all observables and only DM is contributing as a γ-ray source.

The bound corresponding to the IGRB energy spectrum has been derived using the IGRB estimated by the Fermi-LAT Collaboration [27] and adding up in quadrature statistical and systematic errors given in their Table 3. For the autocorrelation bound, we considered the angular spectrum estimated in four energy bins in Ref. [29] as provided in their Table II (DATA:CLEANED) and averaged in the multipole range $155 \leq \ell \leq 504$. For both probes, the model prediction has been computed using the same DM modeling as in our analysis. Our bounds are compatible with the ones presented in Refs. [30–35] (under the same set of assumptions). Cluster bounds are instead taken directly from the literature. In particular, for annihilating DM, we consider the analysis of 34 clusters using expected sensitivity for the five years of Fermi-LAT data in Ref. [36] which uses the same LOW model adopted here. For decaying DM, we consider the analysis of eight clusters in three years of Fermi-LAT data taking performed by [37].

Figure 4 shows that the cross-correlation technique stands out as the most sensitive one, improving the

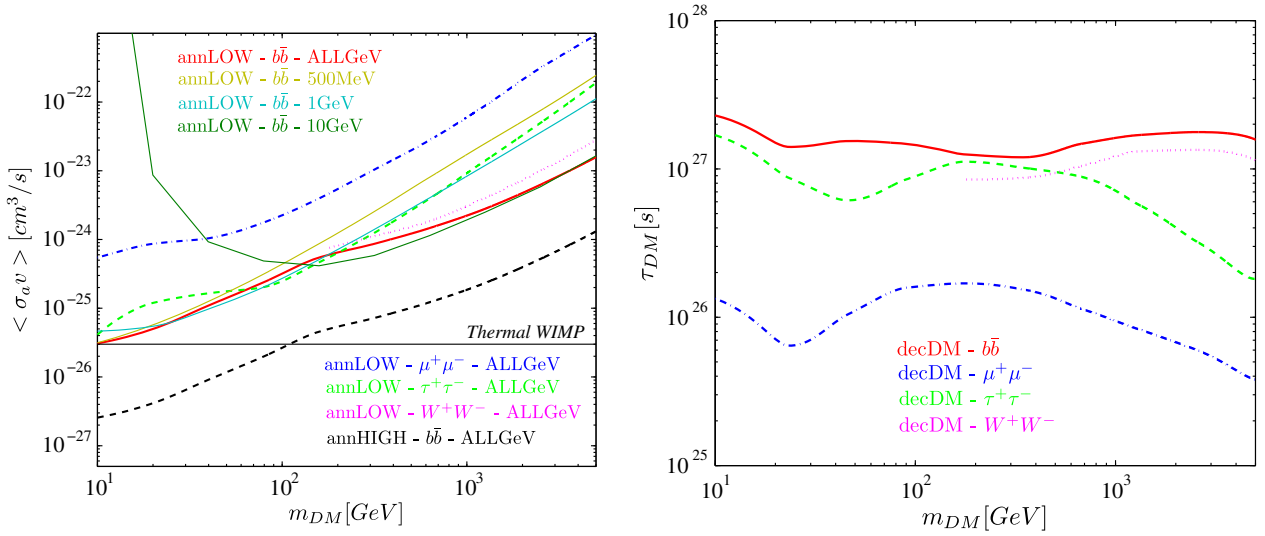

FIG. 3 (color online). Left: 95% C.L. upper limits on the DM annihilation rate as a function of its mass. Both HIGH and LOW clustering schemes are shown for WIMPs annihilating into $b\bar{b}$ (with the impact of different energy bins reported for the latter case). Other final states of annihilation ($\mu^+\mu^-$, $\tau^+\tau^-$, W^+W^-) are shown in the LOW scenario only, for clarity. Right: 95% C.L. lower limits on the DM lifetime as a function of its mass, for different final states of decay.

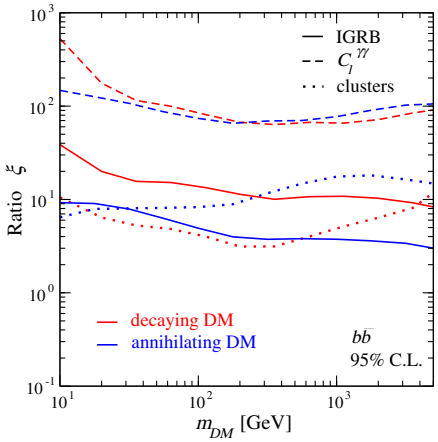

FIG. 4 (color online). Ratio $\xi = \langle\sigma_a v\rangle_i / \langle\sigma_a v\rangle_X$ (in the annihilating DM case) and $\xi = \tau_X/\tau_i$ (in the decaying DM case) between the 95% C.L. bounds derived with the method discussed in this work (cross-correlation of γ rays with the 2MASS catalogue, labeled with X) and from other extragalactic γ-ray probes (i stands for total IGRB intensity, angular autocorrelation, or clusters). The plot refers to the $b\bar{b}$ final state and (for the annihilating DM case) the LOW substructure scheme.

constraints by a factor between a few to a hundred over the other techniques. Note that the ratio decreases at high energy because our analysis focuses at low energies (up to $E > 10$ GeV). Since the IGRB is measured up to 820 GeV there is room for further improvements.

Conclusions.—We compared the predicted angular cross-correlation between the γ-ray emission induced by DM annihilation or decay and the distribution of 2MASS galaxies with the measured CCF between these objects and the Fermi-LAT γ-ray maps.

The contribution of astrophysical sources to the IGRB is assumed to be subdominant at low redshift and not included in the model prediction, in order to derive conservative bounds on DM. We found that in the LOW [25] and HIGH [26] scenarios the "thermal" annihilation cross section is excluded at 95% C.L. up to DM masses of 10 and 100 GeV, respectively, for the final state of annihilation into $b\bar{b}$ and $\tau^+\tau^-$.

We demonstrated that the cross-correlation technique is significantly more sensitive to a DM signal than all other extragalactic γ-ray probes used so far. This was done by comparing the bounds of our cross-correlation analysis with the most recent results from IGRB, angular autocorrelation, and clusters, finding an improvement of a factor ranging from a few up to 100 for both annihilating and decaying DM.

We showed that a WIMP DM contribution can fully explain the observed cross-correlation. A canonical WIMP with a mass in the 10–100 GeV range, an annihilation rate around the thermal value, and a realistic model for DM halo and subhalo properties reproduce both the size and shape of the measured angular cross-correlation. This intriguing possibility deserves further investigation within a more comprehensive framework that include contributions from astrophysical sources and additional data.

A future investigation employing the Pass8 release from the Fermi-LAT and forthcoming surveys at low and intermediate redshift [38] will therefore provide remarkable insights to the particle DM quest.

This work is supported by the PRIN 2012 research grant "Theoretical Astroparticle Physics" No. 2012CPPYP7 funded by MIUR, by the research grants TAsP (Theoretical Astroparticle Physics) and Fermi funded by the INFN, and by the "Strategic Research Grant: Origin and Detection of Galactic and Extragalactic Cosmic Rays," funded by Torino University and Compagnia di San Paolo. J. X. is supported by the National Youth Thousand Talents Program, the National Science Foundation of China under Grant No. 11422323, and the Strategic Priority Research Program, "The Emergence of Cosmological Structures" of the Chinese Academy of Sciences, Grant No. XDB09000000. M. V. and E. B. are supported by PRIN MIUR and IS PD51 INDARK grants. M. V. is also supported by ERC-StG cosmoIGM, PRIN INAF.

*regis@to.infn.it
†xiajq@ihep.ac.cn
‡acuoco@to.infn.it

[1] S. Camera, M. Fornasa, N. Fornengo, and M. Regis, A novel approach in the weakly interacting massive particle quest: Cross-correlation of gamma-ray anisotropies and cosmic shear, Astrophys. J. **771**, L5 (2013).
[2] S. Ando, A. Benoit-Levy, and E. Komatsu, Mapping dark matter in the gamma-ray sky with galaxy catalogs, Phys. Rev. D **90**, 023514 (2014).
[3] N. Fornengo and M. Regis, Particle dark matter searches in the anisotropic sky, Front. Phys. **2**, 6 (2014).
[4] M. Shirasaki, S. Horiuchi, and N. Yoshida, Cross-correlation of cosmic shear and extragalactic gamma-ray background: Constraints on the dark matter annihilation cross-section, Phys. Rev. D **90**, 063502 (2014).
[5] S. Ando, Power spectrum tomography of dark matter annihilation with local galaxy distribution, J. Cosmol. Astropart. Phys. 10 (2014) 061.
[6] S. Camera, M. Fornasa, N. Fornengo, and M. Regis, Tomographic-spectral approach for dark matter detection in the cross-correlation between cosmic shear and diffuse gamma-ray emission, arXiv:1411.4651.
[7] W. B. Atwood *et al.* (LAT Collaboration), The large area telescope on the Fermi gamma-ray space telescope mission, Astrophys. J. **697**, 1071 (2009).
[8] T. H. Jarrett, T. Chester, R. Cutri, S. Schneider, M. Skrutskie, and J. P. Huchra, 2MASS extended source catalog: overview and algorithms, Astron. J. **119**, 2498 (2000).
[9] J. Q. Xia, A. Cuoco, E. Branchini, and M. Viel, Tomography of the Fermi-LAT γ-ray diffuse extragalactic signal via cross

correlations with galaxy catalogs, Astrophys. J. Suppl. Ser. **217**, 15 (2015).
[10] D. N. Limber, Astrophys. J. **117**, 134L(1953); N. Kaiser, Astrophys. J. **388**, 272 (1992); **498**, 26 (1998).
[11] P. A. R. Ade *et al.* (Planck Collaboration), Planck 2015 results. XIII. Cosmological parameters, arXiv:1502.01589.
[12] A. Franceschini, G. Rodighiero, and M. Vaccari, The extragalactic optical-infrared background radiations, their time evolution and the cosmic photon-photon opacity, Astron. Astrophys. **487**, 837 (2008).
[13] J. Q. Xia, A. Cuoco, E. Branchini, M. Fornasa, and M. Viel, A cross-correlation study of the Fermi-LAT γ-ray diffuse extragalactic signal, Mon. Not. R. Astron. Soc. **416**, 2247 (2011).
[14] See Supplemental Material at http://link.aps.org/supplemental/10.1103/PhysRevLett.114.241301, which includes Refs. [15–21], for discussions on: γ-ray bounds from Local Group systems, astrophysical extragalactic backgrounds and uncertainties associated to the DM clustering.
[15] M. Ackermann *et al.* (Fermi-LAT Collaboration), Constraints on the galactic halo dark matter from Fermi-LAT diffuse measurements, Astrophys. J. **761**, 91 (2012).
[16] M. Ackermann *et al.* (Fermi-LAT Collaboration), Searching for dark matter annihilation from Milky Way dwarf spheroidal galaxies with six years of Fermi-LAT data, arXiv:1503.02641.
[17] V. Bonnivard, C. Combet, D. Maurin, and M. G. Walker, Spherical Jeans analysis for dark matter indirect detection in dwarf spheroidal galaxies: Impact of physical parameters and triaxiality, Mon. Not. R. Astron. Soc. **446**, 3002 (2015).
[18] V. Bonnivard, C. Combet, M. Daniel, S. Funk, A. Geringer-Sameth, J. A. Hinton, D. Maurin, J. I. Read *et al.*, Dark matter annihilation and decay in dwarf spheroidal galaxies: The classical and ultrafaint dSphs, arXiv:1504.02048.
[19] G. A. Gómez-Vargas, M. A. Sánchez-Conde, J. H. Huh, M. Peiró, F. Prada, A. Morselli, A. Klypin, D. G. Cerdeño, Y. Mambrini, and C. Muñoz, Constraints on WIMP annihilation for contracted dark matter in the inner galaxy with the Fermi-LAT, J. Cosmol. Astropart. Phys. 10 (2013) 029.
[20] T. Daylan, D. P. Finkbeiner, D. Hooper, T. Linden, S. K. N. Portillo, N. L. Rodd, and T. R. Slatyer, The characterization of the gamma-ray signal from the central milky way: A compelling case for annihilating dark matter, arXiv:1402.6703.
[21] N. Fornengo, L. Perotto, M. Regis, and S. Camera, Evidence of cross-correlation between the CMB lensing and the Γ-ray sky, Astrophys. J. **802**, L1 (2015).
[22] R. K. Sheth and G. Tormen, Large scale bias and the peak background split, Mon. Not. R. Astron. Soc. **308**, 119 (1999).
[23] J. F. Navarro, C. S. Frenk, and S. D. M. White, A universal density profile from hierarchical clustering, Astrophys. J. **490**, 493 (1997).
[24] F. Prada, A. A. Klypin, A. J. Cuesta, J. E. Betancort-Rijo, and J. Primack, Halo concentrations in the standard Λ cold dark matter cosmology, Mon. Not. R. Astron. Soc. **423**, 3018 (2012).
[25] M. A. Sanchez-Conde and F. Prada, The flattening of the concentration-mass relation towards low halo masses and its implications for the annihilation signal boost, Mon. Not. R. Astron. Soc. **442**, 2271 (2014).
[26] L. Gao, C. S. Frenk, A. Jenkins, V. Springel, and S. D. M. White, Where will supersymmetric dark matter first be seen?, Mon. Not. R. Astron. Soc. **419**, 1721 (2012).
[27] M. Ackermann *et al.* (Fermi-LAT Collaboration), The spectrum of isotropic diffuse gamma-ray emission between 100 MeV and 820 GeV, Astrophys. J. **799**, 86 (2015).
[28] M. Fornasa and M. A. Sanchez-Conde, The nature of the diffuse gamma-ray background, arXiv:1502.02866.
[29] M. Ackermann *et al.* (Fermi LAT Collaboration), Anisotropies in the diffuse γ-ray background measured by the Fermi LAT, Phys. Rev. D **85**, 083007 (2012).
[30] M. Ackermann *et al.* (Fermi-LAT Collaboration), Limits on dark matter annihilation signals from the Fermi-LAT 4-year measurement of the isotropic gamma-ray background, arXiv:1501.05464.
[31] M. Ajello *et al.*, The origin of the extragalactic gamma-ray background and implications for dark-matter annihilation, Astrophys. J. **800**, L27 (2015).
[32] M. Di Mauro and F. Donato, Composition of the Fermi-LAT isotropic gamma-ray background intensity: Emission from extragalactic point sources and dark matter annihilations, Phys. Rev. D **91**, 123001 (2015).
[33] S. Ando and K. Ishiwata, Constraints on decaying dark matter from the extragalactic gamma-ray background, J. Cosmol. Astropart. Phys. 05 (2015) 024.
[34] G. A. Gomez-Vargas, A. Cuoco, , T. Linden, M. A. Sánchez-Conde, J. M. Siegal-Gaskins, T. Delahaye, M. Fornasa, E. Komatsu, F. Prada, and J. Zavala (Fermi-LAT Collaboration), Dark matter implications of Fermi-LAT measurement of anisotropies in the diffuse gamma-ray background, Nucl. Instrum. Methods Phys. Res., Sect. A **742**, 149 (2014).
[35] S. Ando and E. Komatsu, Constraints on the annihilation cross section of dark matter particles from anisotropies in the diffuse gamma-ray background measured with Fermi-LAT, Phys. Rev. D **87**, 123539 (2013).
[36] S. Zimmer (for the Fermi-LAT Collaboration), Galaxy clusters with the Fermi-LAT: Status and implications for cosmic rays and dark matter physics, arXiv:1502.02653.
[37] X. Huang, G. Vertongen, and C. Weniger, Probing dark matter decay and annihilation with Fermi-LAT observations of nearby galaxy clusters, J. Cosmol. Astropart. Phys. 01 (2012) 042.
[38] M. Bilicki, T. H. Jarrett, J. A. Peacock, M. E. Cluver, and L. Steward, Two micron all sky survey photometric redshift catalog: a comprehensive three-dimensional census of the whole sky, Astrophys. J. Suppl. Ser. **210**, 9 (2014).